



OPEN ACCESS

EDITED BY

Jing Yu,
Sun Yat-sen University, China

REVIEWED BY

Yaqiang Yang,
Jiangsu University of Science and
Technology, China
Sheng Shen,
Fuzhou University, China

*CORRESPONDENCE

Zhigang Zhang,
zhangzg@cqu.edu.cn

SPECIALTY SECTION

This article was submitted
to Structural Materials,
a section of the journal
Frontiers in Materials

RECEIVED 02 November 2022

ACCEPTED 14 November 2022

PUBLISHED 28 November 2022

CITATION

Sun R, Li Y, Qin F and Zhang Z (2022),
Impedance-based damage assessment
of steel-ECC composite deck using
piezoelectric transducers.
Front. Mater. 9:1087617.
doi: 10.3389/fmats.2022.1087617

COPYRIGHT

© 2022 Sun, Li, Qin and Zhang. This is an
open-access article distributed under
the terms of the [Creative Commons
Attribution License \(CC BY\)](https://creativecommons.org/licenses/by/4.0/). The use,
distribution or reproduction in other
forums is permitted, provided the
original author(s) and the copyright
owner(s) are credited and that the
original publication in this journal is
cited, in accordance with accepted
academic practice. No use, distribution
or reproduction is permitted which does
not comply with these terms.

Impedance-based damage assessment of steel-ECC composite deck using piezoelectric transducers

Rui Sun, Yunjuan Li, Fengjiang Qin and Zhigang Zhang*

Key Laboratory of New Technology for Construction of Cities in Mountain Area, Ministry of Education, School of Civil Engineering, Chongqing University, Chongqing, China

The excellent crack and fatigue resistance of Engineering Cementitious Composites (ECC) materials makes it promising to be used in orthotropic bridge deck system. However, overloading and fatigue load might cause structural damage and, consequently, structural performance degradation. In this work, the piezoelectric lead-zirconate-titanate (PZT) transducers are used to identify the structural damage of the steel-ECC composite deck by implementing both experimental test and numerical simulation. Two steel-ECC composite deck are prepared and four-point bending loading tests are performed on the two specimens to introduce several damage scenarios by gradually increasing the load. The impedance output signals of the piezoelectric sensors are measured under different damage scenarios, and the damage index are extracted to identify the structural damage. A finite element model of the steel-ECC composite deck is established, and the impedance signals with different damage scenarios are calculated and used to assess the structural damages. According to the experimental test and numerical simulation, the impedance-based technology performs to be an effective way to identify the structural damage of the steel-ECC composite deck.

KEYWORDS

steel-ECC composite deck, damage assessment, impedance-based technology, finite element analysis, PZT transducer

Introduction

Orthotropic steel bridge deck is a structural system composed of steel plate stiffened by a series of longitudinal ribs and transversal floor beams that are welded together (Sim and Uang, 2012). Such decks are widely used in long-span bridges because of their high strength-to-weight ratio, high bearing capacities, and convenient construction process (Zhang et al., 2015). However, compared to reinforced concrete decks, the orthotropic steel bridge decks are subjected to considerable local deformations caused by the wheel loads. With the growth of operation time, high local stress amplitude, vehicle overload and other factors easily lead to fatigue damage of steel bridge deck, which has been found many times in the past 3 decades (Shao et al., 2013; Di et al., 2022).

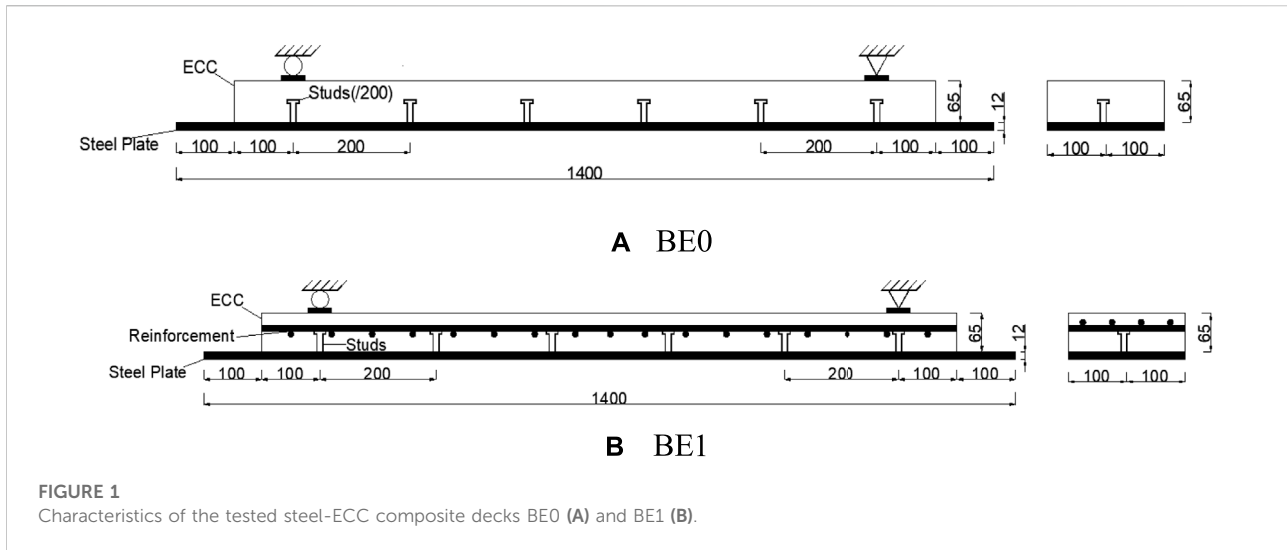


FIGURE 1
Characteristics of the tested steel-ECC composite decks BE0 (A) and BE1 (B).

To mitigate the problem of fatigue damage as it appears in the steel bridge deck, ECC (Engineered Cementitious Composite) was proposed to be used as bridge deck, which is expected to enhance the local stiffness of orthotropic steel bridge deck. ECC is a kind of high ductility concrete with tensile strain capacity exceed 3% (Zhang et al., 2020; Huang et al., 2021; Zhang et al., 2022), which allows it deform with steel bridge deck synergistically. Uniquely, under loadings, the micron-sized cracks develop on ECC other than one single localized cracking that was normally observed in conventional concrete (Yu et al., 2020; Zhang et al., 2021). Such the tiny crack on ECC can heal itself autogeneously under certain conditions (Zhang et al., 2019a), which is expected to prevent the invasion of aggressive agent (i.e., water and chloride ion).

For the composite bridge deck formed by ECC or other ultra-high performance cement-based composites and steel bridge deck, some studies have been carried out. Kakuma et al. (2011) integrated ECC layer and steel bridge deck with studs welded on the steel plate, and found that ECC and steel bridge deck can play a good integral role, and the crack width of ECC can be restricted below 100 μm . Zhao et al. (2019a) investigated the fatigue behavior of steel-ECC composite bridge deck, and found that the ECC layer of exhibited multi-crack cracking performance and high fatigue resistance under fatigue bending test. Guan et al. (2021) found that the cracking stress of ECC layer of steel ECC-composite bridge deck was between 13.4 and 21.0 MPa, and the ECC layer can still bear the flexural load along with steel deck after cracking, which effectively improves the local stiffness of steel bridge deck and reduces the local bending stress amplitude. Zhang et al. (2019b) demonstrated the feasibility of utilization of ECC with self-healing capacity on long-span steel bridge deck, and revealed that the service life of bridge deck can be extended significantly.

However, the performance deterioration of steel-ECC composite deck system might occur due to the long-term temperature effect, fatigue load, and vehicle overloading, which would introduce durability issues, such as crack-induced water invasion and shear resistance decreasing. Therefore, it is of great importance to assess the damage of steel-ECC composite deck to prevent its progress at an early stage, which is essential for the maintenance of bridge in operation.

Piezoelectric transducers (PZT), which has direct and inverse piezoelectric effects, can be used as sensor and actuator simultaneously. It can be embedded into or installed on the surface of structures to detect the changes of structural integrity, that is, often caused by damages (Park et al., 2006; Song et al., 2008). Due to the unique characteristics, i.e. wide frequency range, active sensing and low power consumption, it has been widely used in structural damage detection. The PZT-based structural damage identification methods can be classified as wave propagation and impedance method. The former is to apply electrical excitation on the PZT to emit stress waves, and to evaluate the structural changes by extracting signal features of the collected stress wave signals (i.e., amplitude and energy dissipation), thereby identifying the structural damage (Su et al., 2006; Mitra and Gopalakrishnan, 2016). The basic principle of the impedance method is that the structural damage will cause the change of its mechanical impedance. The mechanical and electrical coupling characteristics of the PZT sensor and the main structure are used to reflect the change of mechanical impedance of the structure through electrical impedance signal of the piezoelectric sensor, so as to identify the structural damage at an early stage (Annamdas and Radhika, 2013; Na and Baek, 2018; Fan et al., 2021).

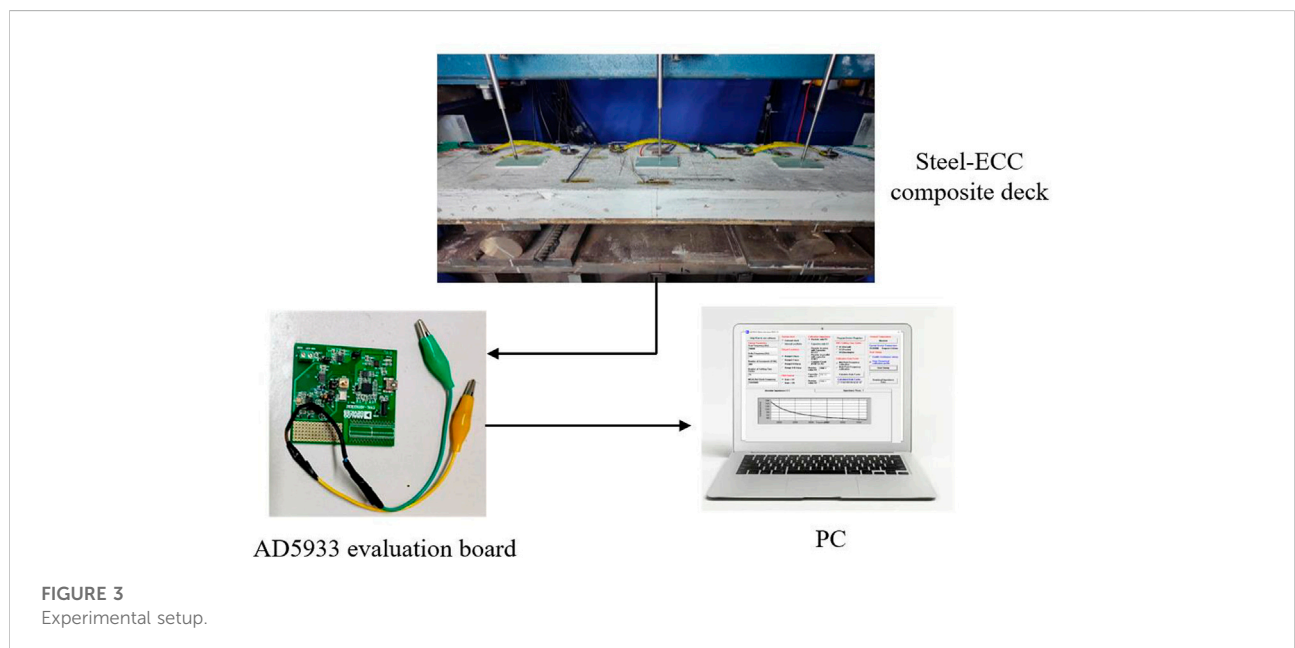
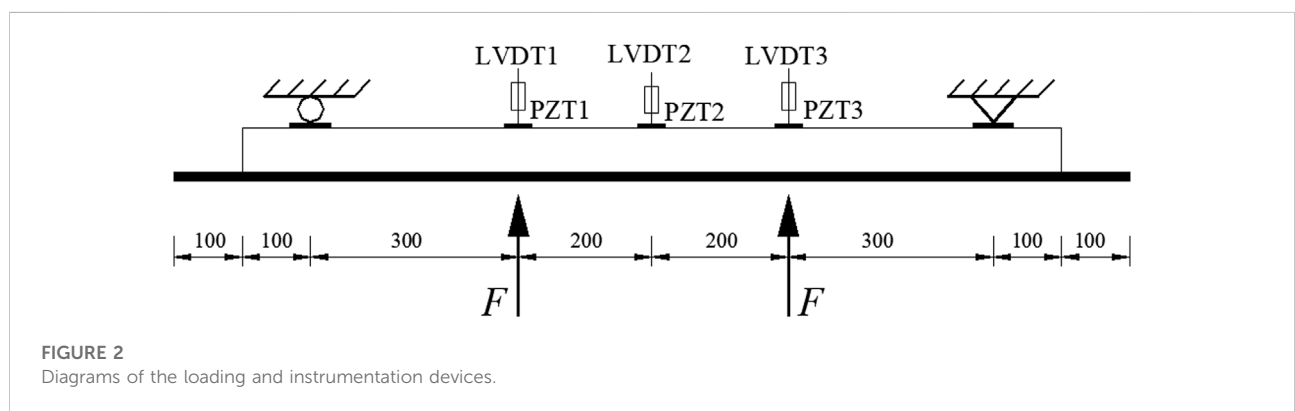
Liang (Liang et al., 1994; Liang et al., 1996) was the first to develop the electro-mechanical impedance model which reveal

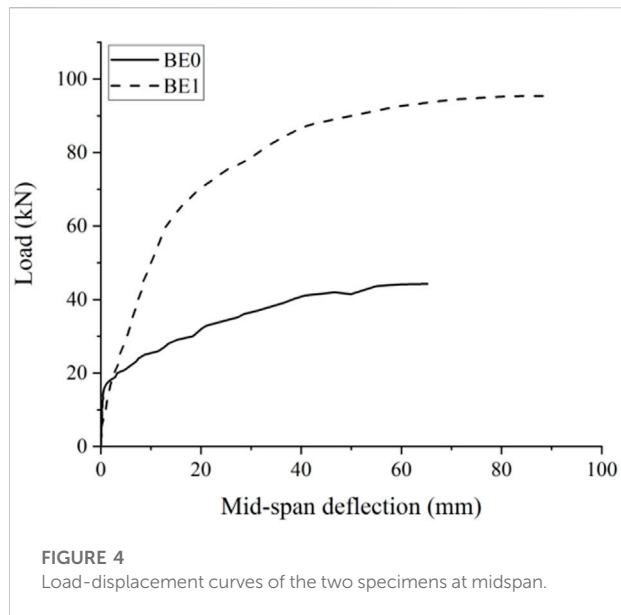
TABLE 1 Parameters of steel-ECC composite deck.

Specimen	Spacing of stubs (mm)	Number of stubs	Number of steel reinforcement	Reinforcement ratio
BE0	200	6	0	0
BE1	200	6	4	2.4%

TABLE 2 ECC mix ratio (kg/m³).

Cement	Fly ash	Silica fume	Limestone powder	Quartz sand	Fibre	Superplasticizer	Water
714.4	451.2	90.99	184.51	451	20	20	275





the coupling of PZT sensor and host structure. Thereafter, the application of impedance-based technique has been widely conducted for damage detection of pipeline system, metallic structure, reinforced concrete, bolted joints and composite structure in the past decades. Surface bonded and embedded PZT sensors were used to detect the cracks, freezing-thawing damage and flexural damage stages of concrete structures (Sabet and Yang, 2014; Karayannis et al., 2015; Liu et al., 2017; Zhao et al., 2020). A good correlation relationship can

TABLE 3 Damage scenarios of steel-ECC composite deck of experimental test.

	Damage scenario	Load (kN)
BE0	D0	0
	D1	10
	D2	20
	D3	30
	D4	40
BE1	D0	0
	D1	20
	D2	40
	D3	60
	D4	80

be observed between the location and severity of structural damages, that is, a closer and severer damage likely induce a higher value of damage indicators, such as root mean square deviation (RMSD), mean absolute percentage deviation (MAPD), covariance, and correlation coefficient (CC) (Giurgiutiu, 2007).

Corrosion of steel structure is identified by using impedance-based technique since it is able to continuously detect variation of the host structure using impedance analyzer. Ai et al. (2014); Zhu et al. (2016) used the admittance (inverse of impedance) signal of PZT sensor to detect the steel corrosion, and the structural damage can be quantified according to the changes of measurements. Li et al.

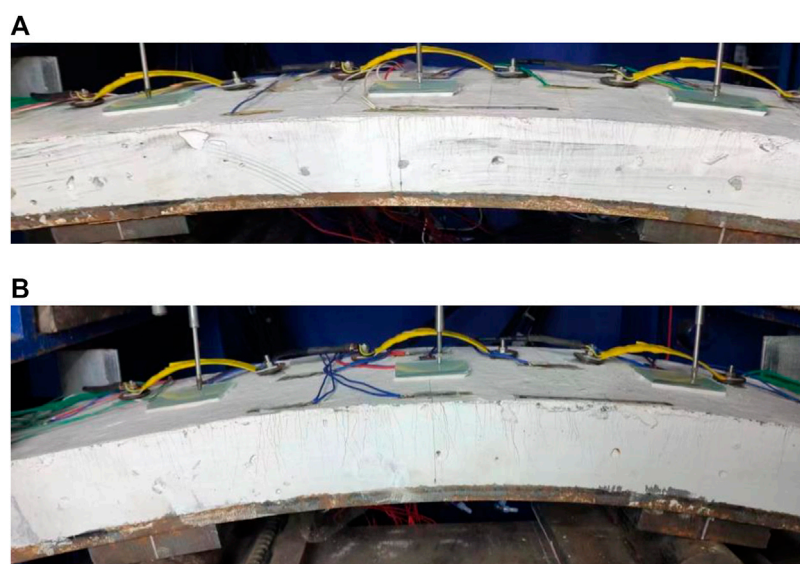
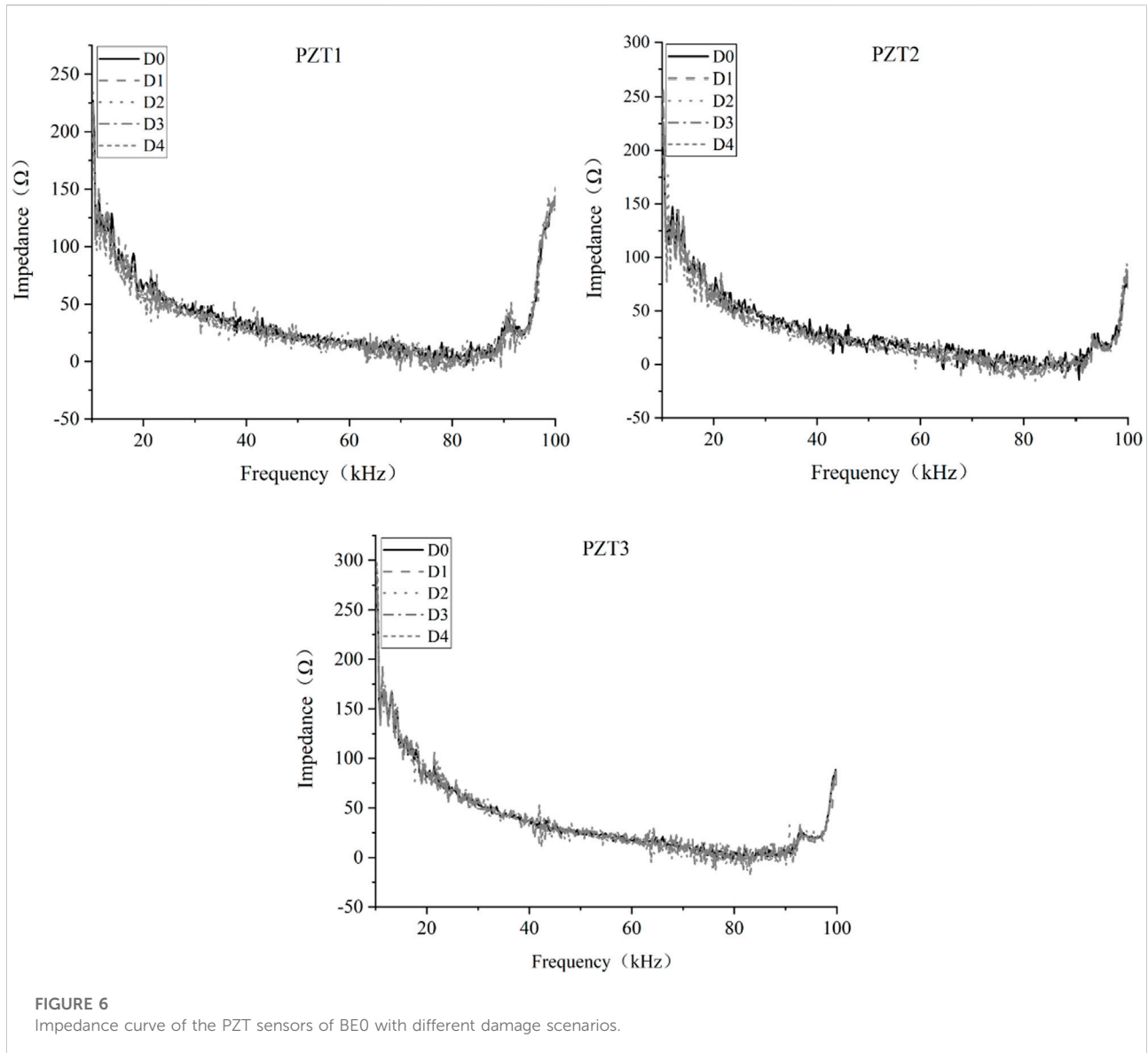
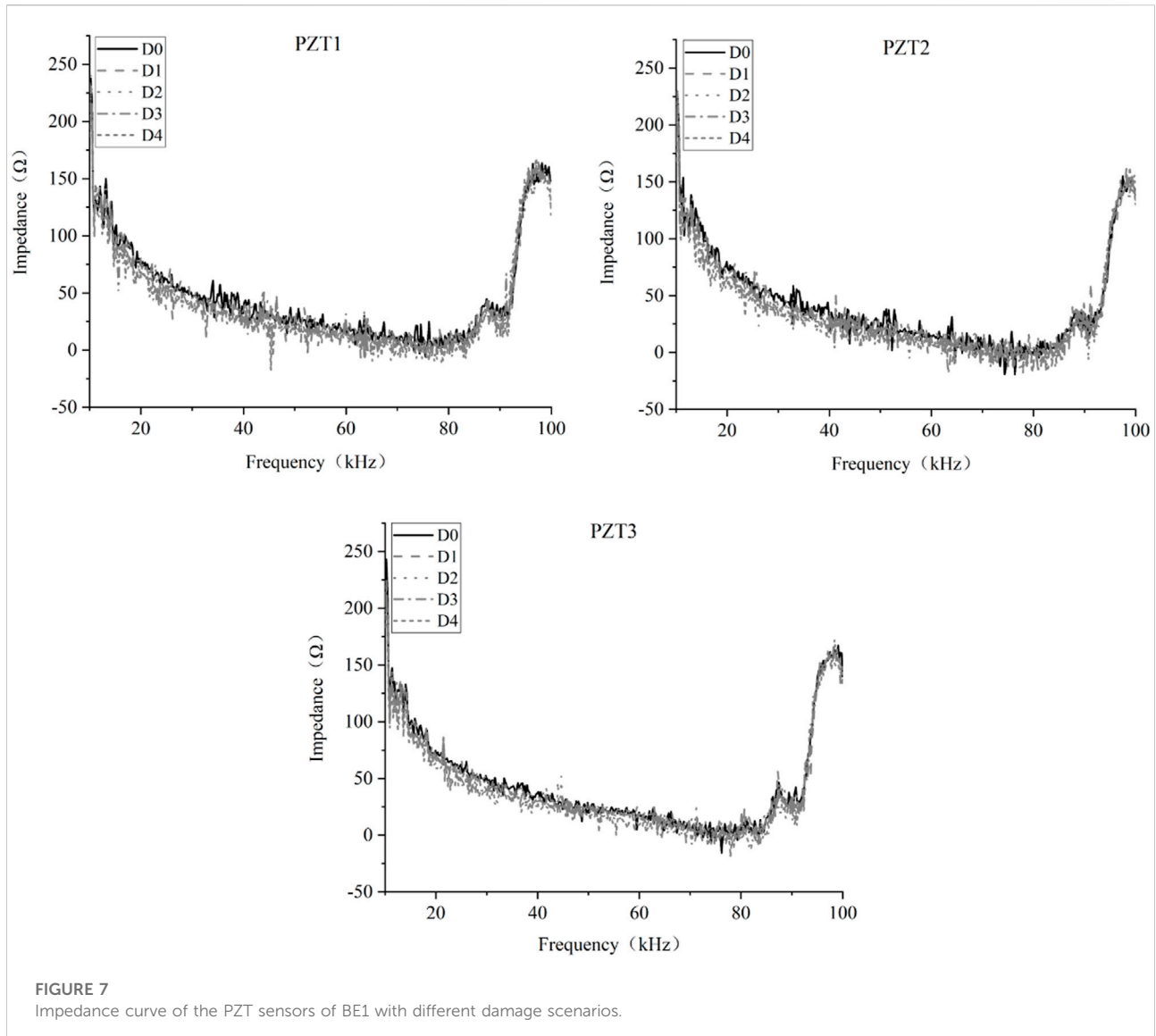


FIGURE 5
Crack distribution of (A) BE0 at 40 kN and (B) BE1 at 80 kN.



(2019) developed a novel corrosion monitoring technique by bonding PZT sensors onto the corrosion coupon using epoxy adhesive, called smart corrosion coupon (SCC). The thickness loss of SCC due to corrosion would lead to the change of impedance signatures, and the corrosion damage can be quantified according to the decrease of frequency peaks and leftward shift of measurements. Due to its capability of continuous monitoring, the impedance-based method is used to monitor the concrete hydration process and strength evaluation (Lim et al., 2016; Negi et al., 2018; Talakokula et al., 2018), which demonstrates that PZT sensors is promising to be used for hydration monitoring of reinforced concrete structures *in situ*. The sensitivity of impedance

signatures to structural damage had been testified due to the high frequency and short wavelength excitation. Therefore, the impedance based method is usually applied for minor defects detection in an early stage, for instance looseness of bolted connection (Nguyen et al., 2017; Li et al., 2020; Na, 2021; Zhou et al., 2021) and interfacial bond damage (Sun et al., 2015; Sun et al., 2017; Deng et al., 2021; Zhu et al., 2022). Furthermore, with the development of artificial intelligence, many studies (Castro et al., 2019; Alazzawi and Wang, 2021; Li et al., 2021; Nguyen et al., 2022; Ai and Cheng, 2023) used machine learning algorithms to cooperate with impedance-based technique, and the capability and accuracy for damage detection and localization are greatly enhanced.



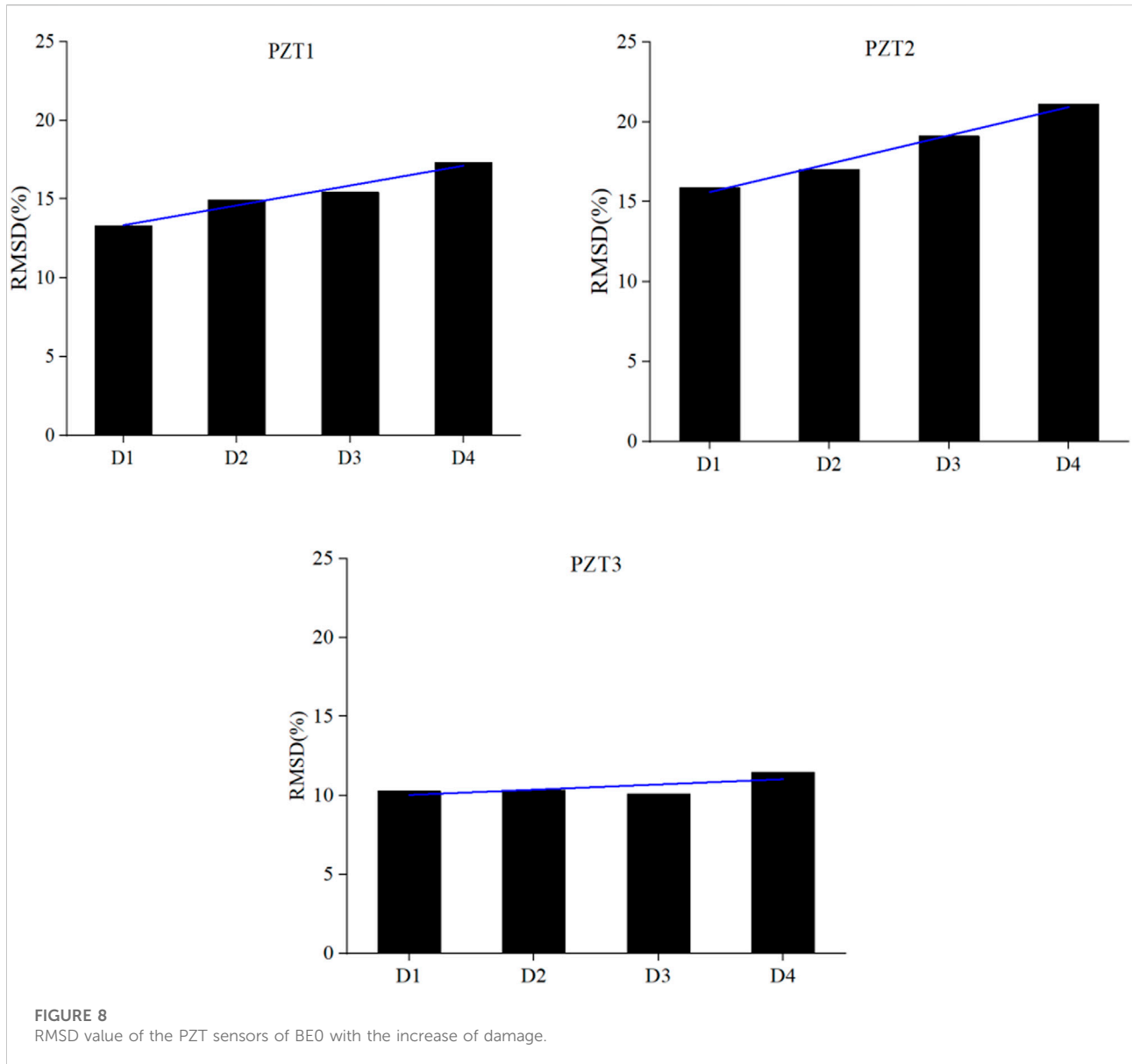
The main objective of this paper is to use impedance-based technique to identify the structural damage of steel-ECC composite deck in a global perspective, which is very difficult to be quantified due to the distribution of amount of micro-cracks in the ECC layer. To achieve this, a four-point loading test is conducted to obtain different damage scenarios of steel-ECC composite deck, and the impedance signals are measured using PZT sensors which were placed on the surface of the specimens. The damage index is extracted from measurements to employ the structural damage identification and localization. Then, the finite element model of the steel-ECC composite deck was established to verify the experimental results. The results showed that the damage of the steel-ECC composite deck can be quantitatively identified based on

the output impedance signal of PZT sensor, and the preliminary location can be obtained.

Experimental setup of steel-ECC composite deck

Specimen details

In this study, two steel-ECC composite decks, named BE0 and BE1, were prepared, which consisted of $1200 \times 200 \times 65$ mm ECC layer and $1400 \times 200 \times 12$ mm Q345 steel deck, and the ECC layer was connected with steel deck by stubs with 13 mm diameter and 35 mm height as shown in Figure 1. Compared with BE0, the ECC layer of BE1 is reinforced with



HRB400 steel mesh. The diameter of steel bars is 10 mm with a spacing of 70 mm, and the thickness of ECC protective layer is 25 mm. The parameters of specimen are shown in Table 1.

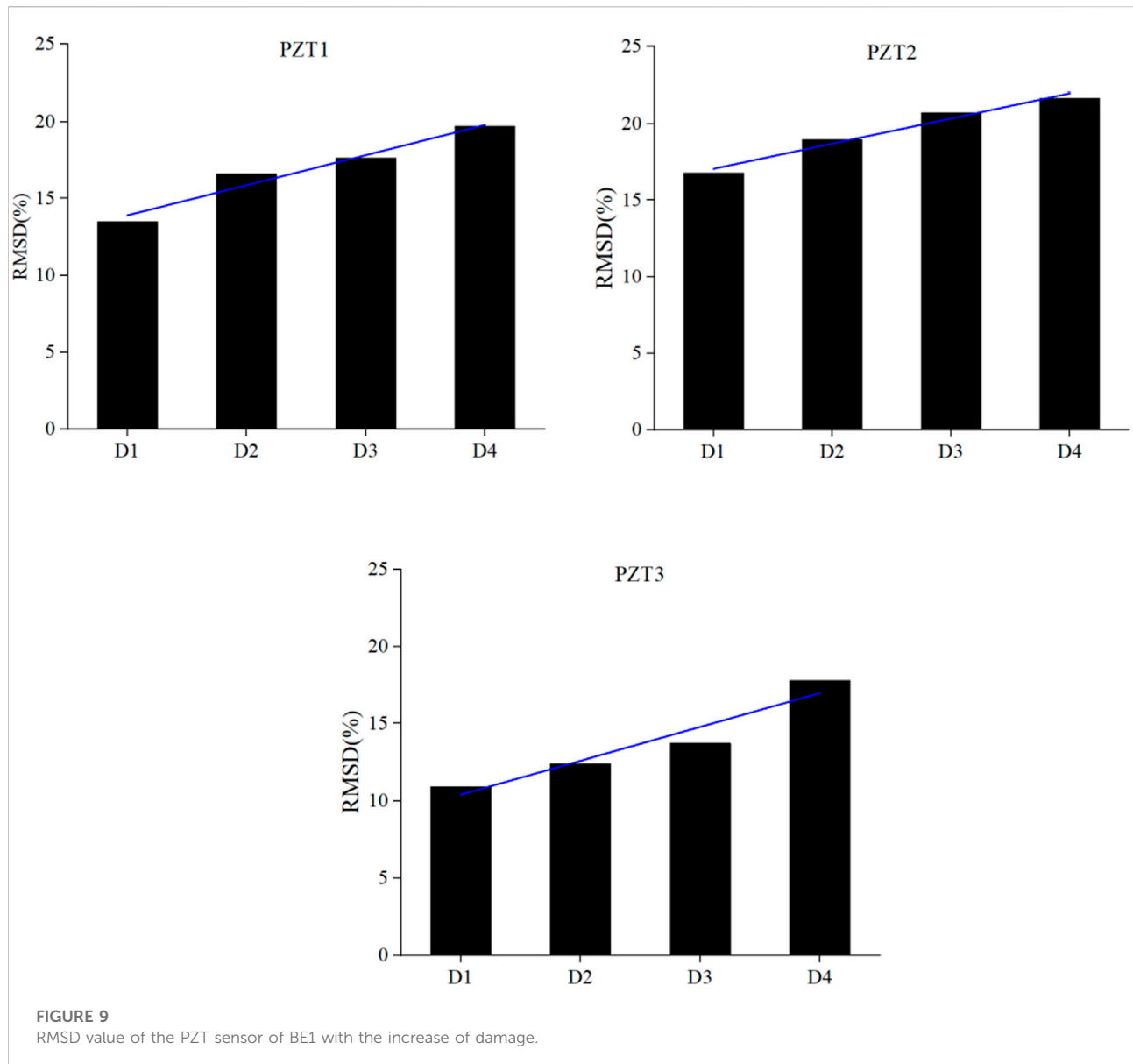
Material properties of ECC layer

The ECC mixture adopted in this study was composed of Portland cement (CEM-52.5), fly ash, silica fume, limestone powder, quartz sand, PE fibres, water and superplasticizer. The mixture proportion of ECC is shown in Table 2. By implementing tensile test for three dog-bone shaped ECC samples, an evident strain-hardening phenomenon can be clearly observed. According to the experimental test, the

average cracking strength of ECC is 4.25 MPa, and the average ultimate tensile strain and ultimate tensile stress of ECC in this study is 4.37% and 9.27 MPa, respectively. In addition, the average compressive strength of ECC is 111.6 MPa.

Test setup and instrumentation

As shown in Figure 2, a four-point loading test was performed on the specimen, and an oil jack was used to control the load which was measured by a load sensor with a maximum range of 500 kN. The load is transferred from the loading point to steel-ECC composite deck specimen through distribution beam, forming a pure bending section with 400 mm



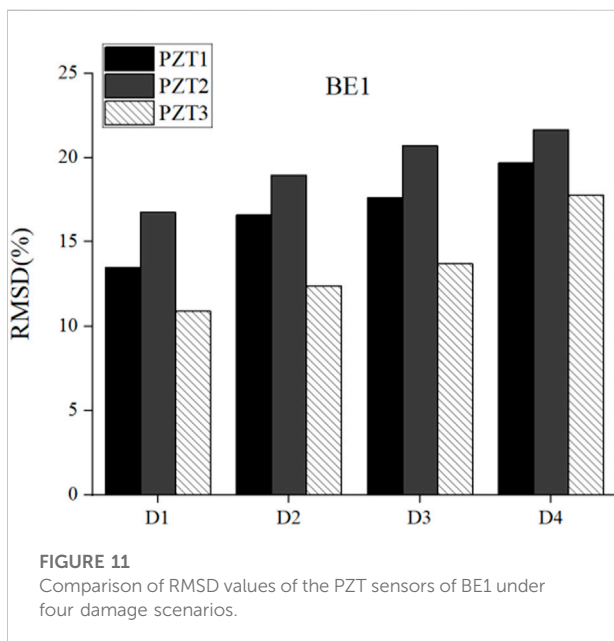
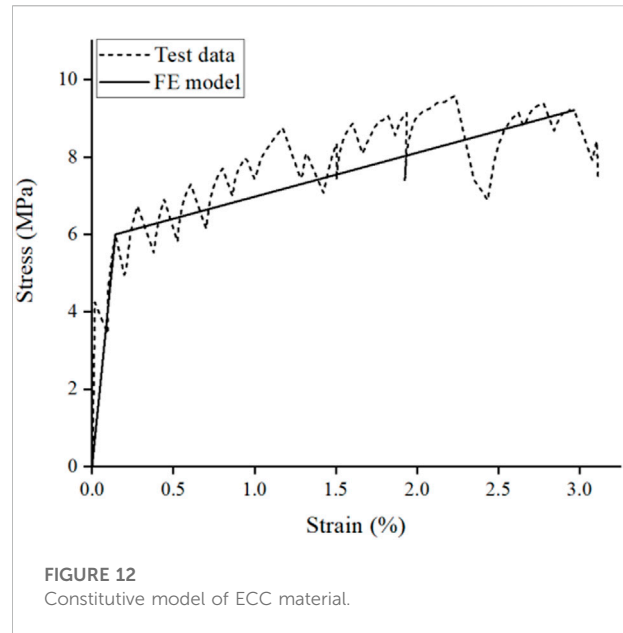
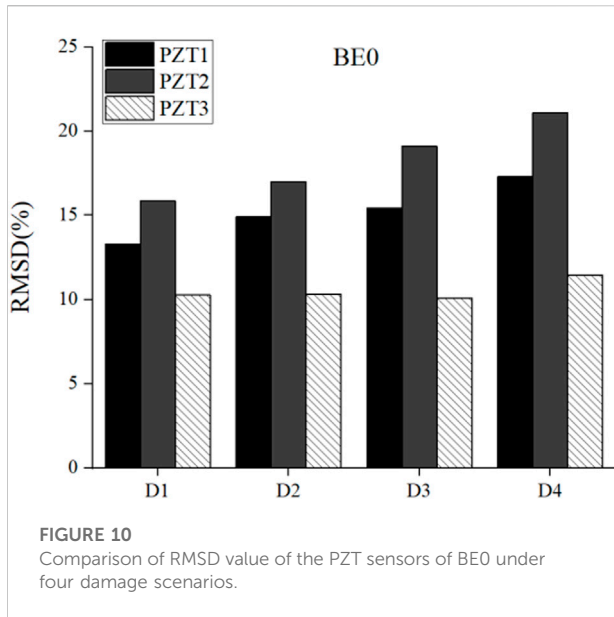
in length on specimen. Three linear variable differential transducers (LVDTs) were arranged at the mid-span section of composite deck and at loading point with a spacing of 200 mm to measure the deflection of specimen during loading process. The strain was recorded by a static data acquisition system.

In order to monitor the different damage states of ECC-deck specimens during, three PZT sensors with dimensions of $10 \times 10 \times 1$ mm were arranged on specimen surface with a spacing of 200 mm, located at 300 mm from two supports of specimen and at the mid-span of the deck, numbered PZT1-PZT3 from left to right, as shown in Figure 2. The electrical impedance signal test was carried out using the AD5933 impedance analysis chip, as shown in Figure 3. During loading process, when the steel-ECC composite deck

is under different damage scenarios induced by different load levels, the output impedance signature of each PZT sensor was tested in the range of 10–100 kHz with 400 frequency sampling points. By doing that, the damage states of the steel-ECC deck can be monitored, since the variation of PZT impedance signature is directly related to the change of structural integrity which implies structural damage.

Experimental results

The load-midspan deflection curves of the two specimens are shown in Figure 4. For BE1, it was initially in the linear elastic stage, and the load was proportional to the mid-span



deflection. After that, cracks started to appear in the ECC layer as the load reached cracking load. The stiffness decreases significantly and the load increases slowly with the growth of the midspan deflection, and the ultimate load of the BE1 specimen is 95.5 kN and the mid-span deflection reaches 90.3 mm. The load-midspan deflection curve of BE0 is similar to that of BE1. Since there is no steel reinforcement, its crack load and ultimate load are 15 and 44.5 kN, respectively, and the corresponding midspan deflection values are 0.5 mm and 65.2 mm. The structural

stiffness gradually decreases as cracks occur in the ECC layer, and its load slowly increases with the increase of midspan deflection until structural failure.

According to the test results of BE0 and BE1, it is clear that the steel bars significantly improve the bearing capacity of the specimens, and the ultimate mid-span deflection values also reflected the excellent ductility of the ECC material. The failure modes of BE0 and BE1 were ECC cracking and steel yielding respectively, nevertheless, there were no obvious wide cracks on specimens during the whole loading process instead of distributed tiny cracks with the maximum width not exceeding 0.08 mm, which shows the excellent crack width-control-ability of ECC.

In this paper, five damage scenarios D0-D4 are predefined, corresponding to the damage states of the specimens under different loading levels. As shown in Table 3, D0 represents the intact state of specimen. D1-D4 of BE0 correspond to the damage states under 10, 20, 30, and 40 kN, while for BE1, they are related to the damage states under 20, 40, 60, and 80 kN, respectively. For the two specimens, the piezoelectric impedance signals under D0-D4 damage states were measured in order to reflect the structural changes induced by the gradually increased load in real case.

Figure 5 shows the crack distribution of BE0 and BE1 in midspan of ECC layer at load level of 40 and 80 kN, respectively. Similar phenomena can be clearly observed for the two specimens that numerous small-width cracks are distributed along the midspan of deck, which indicate the existence of a severe damage at high load level. However, the phenomenological characterization is not enough to quantitatively evaluate the damage conditions and damage

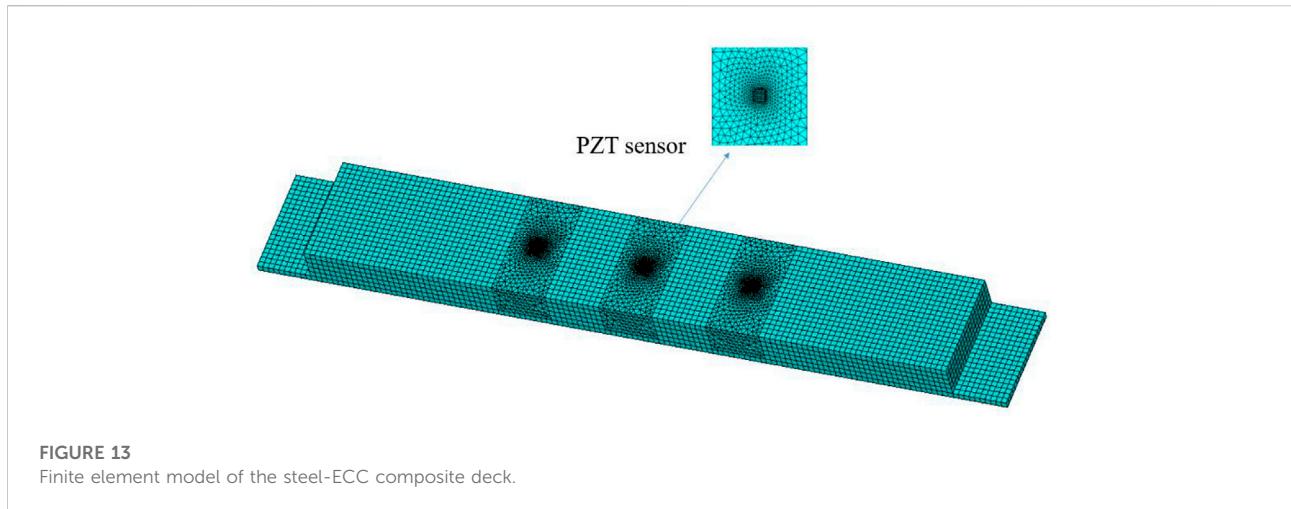


FIGURE 13
Finite element model of the steel-ECC composite deck.

levels of the steel-ECC composite deck since massive micro-cracks would be generated and expanded during the whole process of loading. Despite of this, the impedance-based method provides an effective way to identify structural damage of steel-ECC composite deck, and thereby assess the deterioration of structural performance according to the impedance signals and extracted damage indicator which are directly related to the variation of structural integrity.

As shown in Figure 6 and Figure 7, the impedance signals were tested by PZT1–PZT3 of the specimens BE0 and BE1 under different damage scenarios. From the figures, it can be seen that the impedance signals of the structure in the D1–D4 damage states all changed compared to the healthy state D0, which reflects the variation of structural integrity caused by the load. In order to quantitatively assess the structural damage, the statistical metric RMSD (root mean square derivation) is used as the damage indicator of structure, and its expression is as follows:

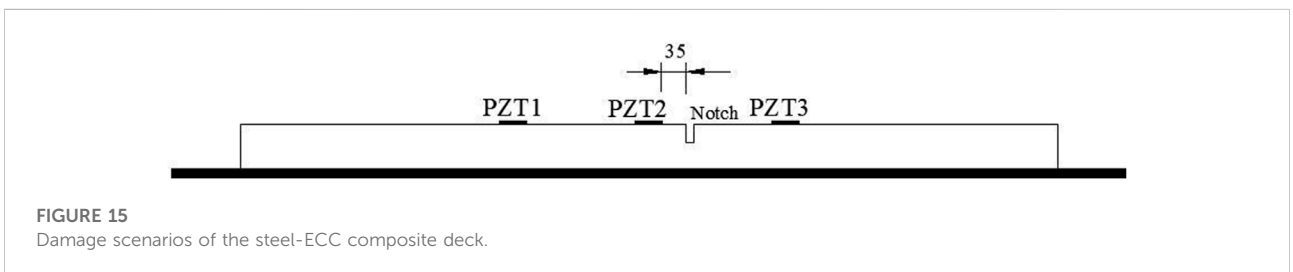
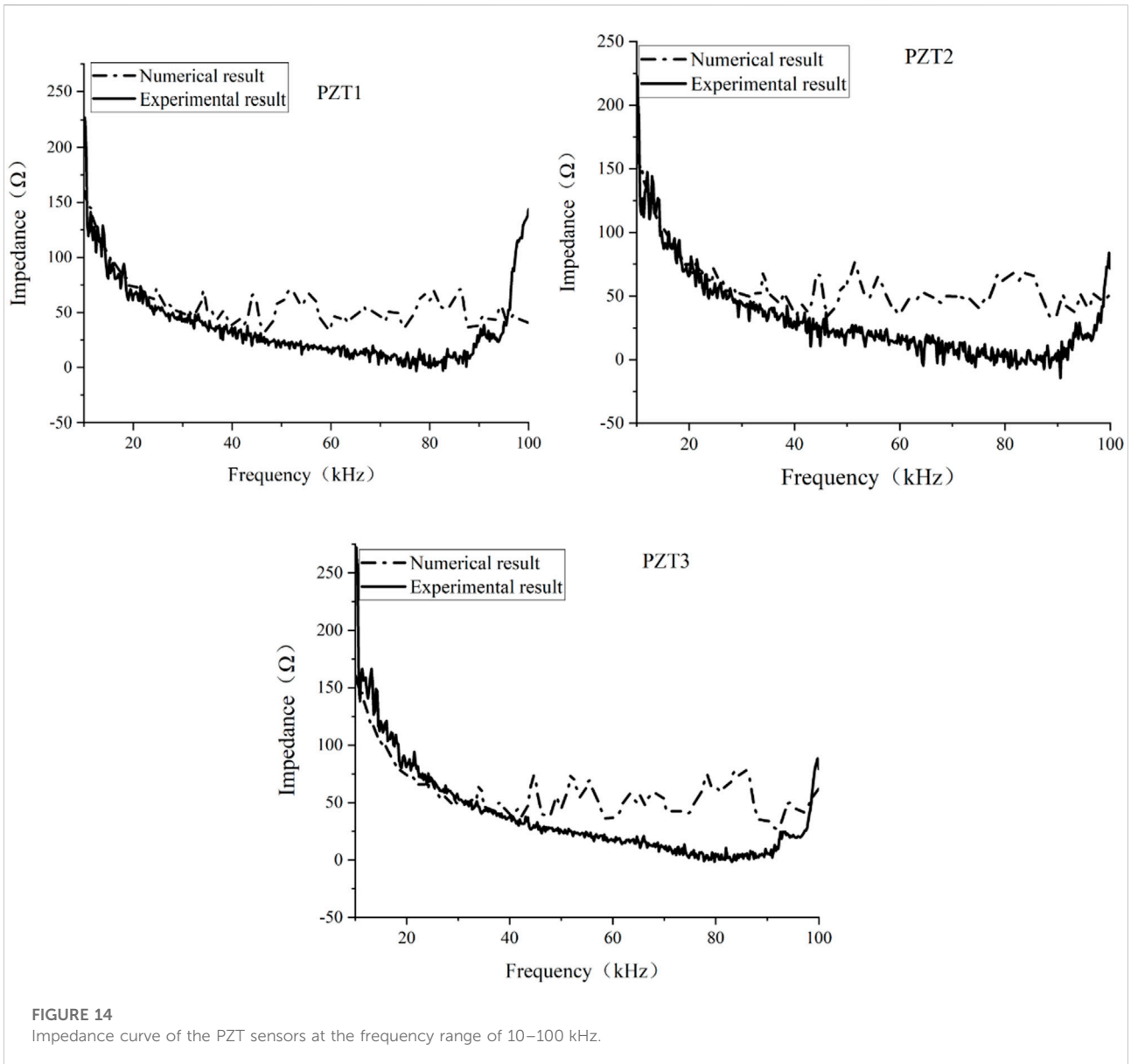
$$RMSD = \sqrt{\frac{\sum_{i=1}^{i=N} (Z_i - Z_0)^2}{\sum_{i=1}^{i=N} Z_0^2}} \quad (1)$$

where Z_0 is the impedance signal in the intact state. Z_i represents the impedance signal in the damage state, i is the measured point in the frequency range. N is the total number of measured points. The value of RMSD is between 0 and 1. When RMSD is equal to 0, it represents the intact state. The larger the value, the larger the deviation between the impedance measurements and the reference measurements (D_0 state), that is, the greater the damage of structure. Based on that, it makes the impedance-based methodology be a physical model-free approach to quantify the structural damage since only impedance measurements of different damage states are needed. And then, the evolution of structural damage can be captured according to the damage index value.

Figure 8 and Figure 9 show the RMSD values of the three PZT sensors bonded on the surface of the two specimens under different damage scenarios. At the elastic stage D1, it can be seen that the RMSD value is relatively small. The RMSD values of the three PZT sensors distributed on the surface of BE0, from PZT1 to PZT3, are 0.133, 0.158, and 0.102, respectively. And the RMSD value of PZT1, PZT2 and PZT3 of BE1 are 0.135, 0.168, and 0.109, respectively. This clearly shows that the PZT sensor is very sensitive to the minor structural damage at an early damage stage, and the change of the structure can be detected quantitatively according to the change of impedance signal.

As shown in Figure 8 and Figure 9, the structural damages of steel-ECC composite decks continues to increase as the load increasing, and the RMSD value of each PZT sensor ascends from D1 to D4. For D4 damage scenario, the RMSD value of PZT1, PZT2, and PZT3 of BE0 reach 0.173, 0.211 and 0.114, respectively. And those of BE1 reach 0.197, 0.217, and 0.178, respectively. It is clear that the RMSD value can directly reflect the change of structural integrity, and the evolution of structural damages with the increase of load can be addressed based on the fact that RMSD value is proportional to the severity of structural damage as shown in Figure 8 and Figure 9. Besides, the RMSD value of the PZT3 sensor of BE0 decreases slightly under the damage conditions of D2 and D3, which might be caused by test errors and environmental noise. Nevertheless, by using the externally bonded PZT sensors, the damage conditions of steel-ECC composite deck can be identified according to the damage index extracted from impedance signals that directly related to the structural damage.

Figure 10 and Figure 11 compare the RMSD value of the three distributed PZT sensors of the two specimens under different damage scenarios. It can be observed that RMSD value of the PZT2 is higher than that of PZT1 and PZT3. Considering that PZT2 is placed in the mid-span of the steel-



ECC composite deck, this indicates that the damage has probably reached more severely in the middle section of specimens. As shown in Figure 5, most of the cracks are distributed along the

midspan section of the deck where PZT2 is located. The number of cracks in the area near two supports is much less than that in the midspan area, where PZT1 and PZT3 are located. This

TABLE 4 Damage scenarios of steel-ECC composite deck for numerical simulation.

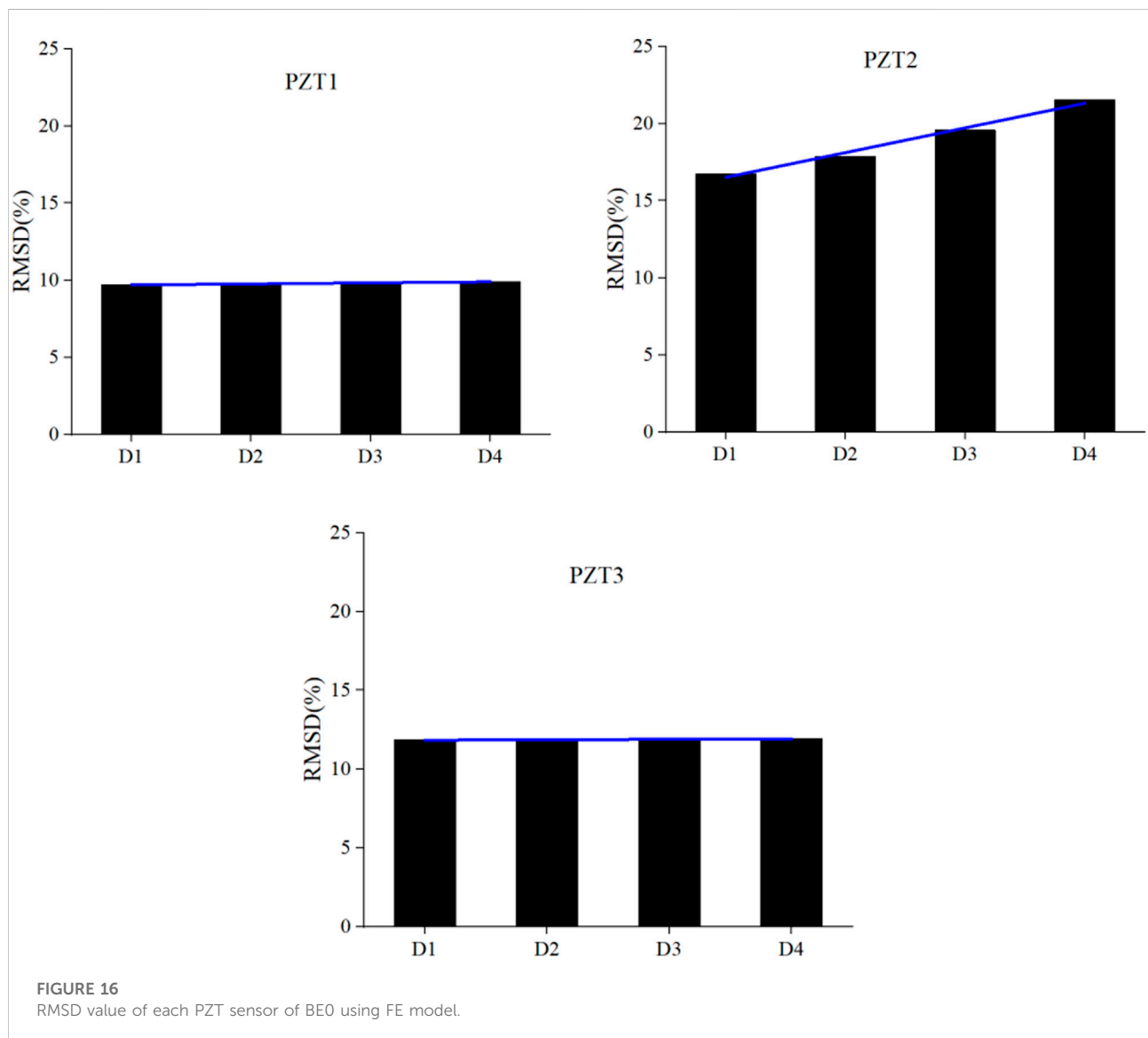
Damage scenarios	Notch depth (mm)
D1	5
D2	10
D3	15
D4	20

phenomenon is consistent with the distribution of RMSD value of the PZT transducers placed on the surface of the steel-ECC composite deck as shown in Figure 10 and Figure 11. Obviously, it implies that the PZT sensor in more severely damaged area is more influenced than the others, leading to a bigger RMSD value.

Therefore, according to the comparison of the damage index of the distributed PZT sensors, it can be found that the RMSD value of the PZT sensor is higher at the location, where the damage severity is higher. The distribution of structural damages of the steel-ECC composite deck can be globally determined using PZT sensors.

Finite element analysis

To verify the effectiveness of the PZT sensor for damage identification of the steel-ECC deck structure, the BE0 specimen was selected to establish a finite element model and implement numerical simulation using commercial finite element software ANSYS. SOLID 45 and SOLID 65 were introduced to represent the steel plate and the ECC layer. SOLID5 was used to simulate



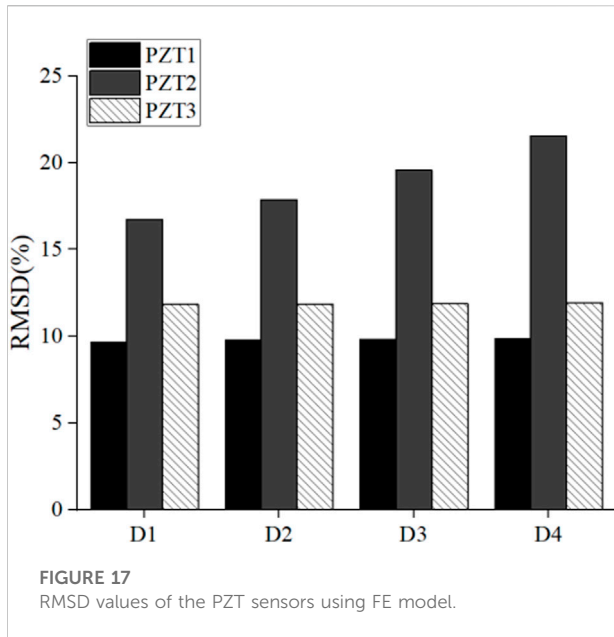


FIGURE 17
RMSD values of the PZT sensors using FE model.

the electro-mechanical coupling effect of PZT sensor. Since the amplitude of the excitation of PZT transducer is very small compared to the structural deformation, the interfacial bond-slip between PZT and the host structure is ignored, and a perfect bond model is adopted in order to simplify the process of numerical simulation. The material properties of ECC and steel used in the FE model are consistent with the experimental test. As shown in Figure 12, the yield and ultimate stress of ECC are 6.03 and 9.27 MPa, and the related strains are 0.15% and 2.96%, respectively. The finite element model conducted in this paper is shown in Figure 13.

In this paper, in order to capture the impedance signal in high frequency range, usually higher than 10 kHz, a refined mesh is adopted, especially in the vicinity of PZT sensors. A harmonic voltage signal of 2 V is applied on the upper and lower surfaces of each PZT sensor, and the piezoelectric impedance spectrum curve can be obtained under the excitation of the electrical signal. To verify the established FE model, the electrical impedance signal of each PZT sensor under the intact state is first calculated. Figure 14 shows the comparison of impedance signal between the FE model and that of the test data. Although there is a deviation in the high frequency range of 50–100 kHz, the numerical results agree quite well with the test data, which verifies the accuracy and validity of the finite element model established in this work.

In the experimental test, four damage scenarios were introduced gradually with the increase of load, resulting in a large number of distributed small-width cracks. In order to conveniently simulate different damage severities of steel-ECC composite deck, a notch with a width of 3 mm was artificially introduced to the FE model at a distance of 35 mm from the right side of the PZT2, as shown in Figure 15. Four damage scenarios, D1–D4, were defined by changing

the depth of the notch as shown in Table 4. By applying electrical excitation on the surface of PZT transducer, the impedance signatures can be captured under four damage scenarios.

The impedance output signals of the sensors PZT1–PZT3 in the frequency range of 10–100 kHz under the no-damage and D1–D4 damage scenarios of the steel-ECC composite deck were calculated using FE model. The changes of impedance signals caused by the structural damages are observed which indicates the change of the structural integrity will affect the mechanical impedance of the structure, which will directly lead to the change of the electrical impedance signal of the externally bonded PZT sensor. The RMSD value of the PZT1–PZT3 sensors under different damage scenarios are evaluated in order to quantitatively analyze the influence of structural damage on the impedance signal of the piezoelectric sensor. As shown in Figure 16, from D1 to D4, the RMSD values of the three PZT sensors gradually increase with the increase of the load. Obviously, the change of the structural damage could be directly reflected based on the RMSD value which is proportional to the increase of the damage. Besides, the change of RMSD value of PZT2 with the change of structural damage is more significant than that of PZT1 and PZT3, which indicates that the PZT sensor placed near the damage region is more sensitive to the change of structural damage.

Figure 17 shows the distribution of RMSD values for the three piezoelectric sensors in D1–D4 damage scenarios. It is clear that the RMSD value of PZT2 is significantly higher than that of PZT1 and PZT3, that is, the sensor with a higher value of damage index is closer to the structural damage. Furthermore, the damage is located at the left side of PZT2, which is closer to PZT3 than PZT1, and the RMSD value of PZT3 is obviously higher than that of PZT1 as shown in Figure 17. This phenomenon indicates that a more severe damage might exist in the vicinity of PZT2 and PZT3. Furthermore, it should be noted that a notch is introduced in the FE model to represent the structural damage instead of a large number of tiny-width cracks in the test. Nevertheless, according to the FE analysis and experimental test, it can be concluded that a higher RMSD value of PZT sensor corresponds to a more severe damage nearby. Hence, based on the value of the damage index of the PZT sensors bonded on the structure, the area of the structural damage can be identified in a first step. More PZT sensors would be helpful to assess and localize the damages of steel-ECC composite deck by using impedance measurements under different damage scenarios.

Conclusion

In this paper, the damage identification of steel-ECC composite deck is implemented using piezoelectric sensors. The experimental test includes two steel-ECC composite decks subjected to four-point loading test until failure. A

harmonic voltage excitation is applied on the three PZT sensors externally bonded on the surface of two specimens, and the impedance signals are simultaneously measured at different damage levels induced by gradually increased loading. To assess the structural damages, the statistical damage index RMSD are extracted between the baseline signals in healthy state and related loading/damage level to represent the changes of structural integrity. Further, FE simulation has been carried out to evaluate the impedance signatures of different damage scenarios. The capability of the impedance-based technique for damage identification of the steel-ECC composite deck is verified. Based on that, several conclusions can be drawn:

- 1) Based on the experimental test of steel-ECC composite deck, it can be found that the structural performance is significantly improved by the ECC layer. The maximum crack width of the ECC layer is less than 0.08 mm, so the corrosion of steel is able to be prevented effectively which makes it promising for engineering application under aggressive environments.
- 2) The main advantages of the impedance-based method are that no physical model is required making it a data-driven approach, and the high sensitivity for minor defects according to the high frequency excitation. Hence, it is very convenient and powerful to monitor the health condition of steel-ECC composite deck using impedance signatures of different damage scenarios measured by PZT transducers.
- 3) According to the impedance measurements, the growth of damage severities would result in the increase of damage index RMSD, which makes it be proportional to the structural damage. Therefore, impedance-based technique can be used to directly evaluate the damage conditions of steel-ECC composite deck, and specific values can be determined as early-warning thresholds.
- 4) The impedance signals of PZT sensor is more sensitive to the structural damage in its vicinity, so the region of damage is able to be identified in a first step. For future work, an array of PZT sensors might be used to assess the damage area according to the comparison of damage index value of each sensor based on impedance measurements.

References

- Ai, D., and Cheng, J. B. (2023). A deep learning approach for electromechanical impedance based concrete structural damage quantification using two-dimensional convolutional neural network. *Mech. Syst. Signal Process.* 183, 109634. doi:10.1016/j.ymsp.2022.109634
- Ai, D., Zhu, H. P., Luo, H., and Yang, J. (2014). An effective electromechanical impedance technique for steel structural health monitoring. *Constr. Build. Mater.* 73, 97–104. doi:10.1016/j.conbuildmat.2014.09.029
- Alazzawi, O., and Wang, D. (2021). Damage identification using the PZT impedance signals and residual learning algorithm. *J. Civ. Struct. Health Monit.* 11, 1225–1238. doi:10.1007/s13349-021-00505-9
- Annamdas, V. G. M., and Radhika, M. A. (2013). Electromechanical impedance of piezoelectric transducers for monitoring metallic and non-metallic structures: A review of wired, wireless and energy-harvesting methods. *J. Intelligent Material Syst. Struct.* 24 (9), 1021–1042. doi:10.1177/1045389x13481254
- Castro, B. A., Baptista, F. G., and Ciampa, F. (2019). Comparative analysis of signal processing techniques for impedance-based SHM applications in noisy environments. *Mech. Syst. Signal Process.* 126, 326–340. doi:10.1016/j.ymsp.2019.02.034
- Deng, J., Li, X. D., Zhu, M. C., Rashid, K., and Wang, Q. (2021). Debonding damage detection of the CFRP-concrete interface based on piezoelectric ceramics by the electromechanical impedance method. *Constr. Build. Mater.* 303, 124431. doi:10.1016/j.conbuildmat.2021.124431
- Di, J., Wang, J., Zhou, X. H., Peng, X., and Qin, F. (2022). Fatigue behavior of rib-to-floor beam junctions with separate inner stiffeners in orthotropic steel bridge decks. *J. Bridge Eng.* 27 (5), 04022019. doi:10.1061/(ASCE)BE.1943-5592.0001857
- Fan, X., Li, J., and Hao, H. (2021). Review of piezoelectric impedance based structural health monitoring: Physics-based and data-driven methods. *Adv. Struct. Eng.* 24, 3609–3626. doi:10.1177/13694332211038444

Data availability statement

The original contributions presented in the study are included in the article/Supplementary Material, further inquiries can be directed to the corresponding author.

Author contributions

Conceptualization: RS and ZZ; data curation: YL and FQ; writing original manuscript: RS and FQ; review and editing manuscript: ZZ; funding acquisition: RS, FQ, and ZZ.

Funding

This research was funded by the National Natural Science Foundation of China (No. 52192663, 52078081), the 111 Project of China (Grant No. B18062), the Fundamental Research Funds for the Central Universities (No. 2021CDJQY-039, 2021CDJQY-008), and Chongqing Research Program of Basic Research and Frontier Technology (No. cstc2020jcyjmsxmX0946).

Conflict of interest

The authors declare that the research was conducted in the absence of any commercial or financial relationships that could be construed as a potential conflict of interest.

Publisher's note

All claims expressed in this article are solely those of the authors and do not necessarily represent those of their affiliated organizations, or those of the publisher, the editors and the reviewers. Any product that may be evaluated in this article, or claim that may be made by its manufacturer, is not guaranteed or endorsed by the publisher.

- Giurgiutiu, V. (2007). *Structural health monitoring: With piezoelectric wafer active sensors*[M]. Amsterdam, Netherlands: Elsevier.
- Guan, Y. H., Wu, J. J., Sun, R. J., Zhang, H., Hu, Y., and Wang, F. (2021). Transverse flexural behaviour of steel-Engineering Cementitious Composites (ECC) compo-site deck under negative and positive bending forces. *KSCE J. Civ. Eng.* 25 (8), 2962–2973. doi:10.1007/s12205-021-1053-2
- Huang, B. T., Wu, J. Q., Yu, J., Dai, J. G., Leung, C. K., and Li, V. C. (2021). Seawater sea-sand engineered/strain-hardening cementitious composites (ECC/SHCC): Assessment and modeling of crack characteristics. *Cem. Concr. Res.* 140, 106292. doi:10.1016/j.cemconres.2020.106292
- Kakuma, K., Matsumoto, T., Hayashikawa, T., and He, X. (2011). Fatigue analysis of ECC-steel composite deck under wheel trucking load. *Procedia Eng.* 14, 1838–1844. doi:10.1016/j.proeng.2011.07.231
- Karayannis, C. G., Voutetaki, M. E., Chalioris, C. E., Providakis, C. P., and Angeli, G. M. (2015). Detection of flexural damage stages for RC beams using piezoelectric sensors (PZT). *Smart Struct. Syst.* 15, 997–1018. doi:10.12989/sss.2015.15.4.997
- Li, H., Ai, D., Zhu, H., and Luo, H. (2021). Integrated electromechanical impedance technique with convolutional neural network for concrete structural damage quantification under varied temperatures. *Mech. Syst. Signal Process.* 152, 107467. doi:10.1016/j.ymsp.2020.107467
- Li, N., Wang, F. R., and Song, G. B. (2020). Monitoring of bolt looseness using piezoelectric transducers: Three-dimensional numerical modeling with experimental verification. *J. Intelligent Material Syst. Struct.* 31 (6), 911–918. doi:10.1177/1045389x20906003
- Li, W., Liu, T., Zou, D., Wang, J., and Yi, T. H. (2019). PZT based smart corrosion coupon using electromechanical impedance. *Mech. Syst. Signal Process.* 129, 455–469. doi:10.1016/j.ymsp.2019.04.049
- Liang, C., Sun, F. P., and Rogers, C. A. (1994). Coupled electro-mechanical analysis of adaptive material systems-determination of the actuator power consumption and system energy transfer. *J. Intelligent Material Syst. Struct.* 5, 12–20. doi:10.1177/1045389x9400500102
- Liang, C., Sun, F. P., and Rogers, C. A. (1996). Electro-mechanical impedance modeling of active material systems. *Smart Mat. Struct.* 5, 171–186. doi:10.1088/0964-1726/5/2/006
- Lim, Y. Y., Kwong, K. Z., Liew, W. Y. H., and Soh, C. K. (2016). Non-destructive concrete strength evaluation using smart piezoelectric transducer—a comparative study. *Smart Mat. Struct.* 25, 085021. doi:10.1088/0964-1726/25/8/085021
- Liu, P., Wang, W., Chen, Y., Feng, X., and Miao, L. (2017). Concrete damage diagnosis using electromechanical impedance technique. *Constr. Build. Mater.* 136, 450–455. doi:10.1016/j.conbuildmat.2016.12.173
- Mitra, M., and Gopalakrishnan, S. (2016). Guided wave based structural health monitoring: A review. *Smart Mat. Struct.* 25, 053001. doi:10.1088/0964-1726/25/5/053001
- Na, W. (2021). Bolt loosening detection using impedance based non-destructive method and probabilistic neural network technique with minimal training data. *Eng. Struct.* 226, 111228. doi:10.1016/j.engstruct.2020.111228
- Na, W. S., and Baek, J. D. (2018). A review of the piezoelectric electromechanical impedance based structural health monitoring technique for engineering structures. *Sensors* 18, 1307. doi:10.3390/s18051307
- Negi, P., Chakraborty, T., Kaur, N., and Bhalla, S. (2018). Investigations on effectiveness of embedded PZT patches at varying orientations for monitoring concrete hydration using EMI technique. *Constr. Build. Mater.* 169, 489–498. doi:10.1016/j.conbuildmat.2018.03.006
- Nguyen, T. C., Huynh, T. C., Yi, J. H., and Kim, J. T. (2017). Hybrid bolt-loosening detection in wind turbine tower structures by vibration and impedance responses. *Wind Struct.* 24, 385–403. doi:10.12989/was.2017.24.4.385
- Nguyen, T. T., Phan, T. T. V., Ho, D. D., Man Singh Pradhan, A., and Huynh, T. C. (2022). Deep learning-based autonomous damage-sensitive feature extraction for impedance-based pre-stress monitoring. *Eng. Struct.* 259, 114172. doi:10.1016/j.engstruct.2022.114172
- Park, G., Farrar, C. R., di Scalea, F. L., and Coccia, S. (2006). Performance assessment and validation of piezoelectric active-sensors in structural health monitoring. *Smart Mat. Struct.* 15 (6), 1673–1683. doi:10.1088/0964-1726/15/6/020
- Sabet, D. B., and Yang, Y. (2014). Combined embedded and surface-bonded piezoelectric transducers for monitoring of concrete structures. *NDT E Int.* 65, 28–34. doi:10.1016/j.ndteint.2014.03.009
- Shao, X., Yi, D., Huang, Z., Zhao, H., Chen, B., and Liu, M. (2013). Basic performance of the composite deck system composed of orthotropic steel deck and ultrathin RPC layer. *J. Bridge Eng.* 18 (5), 417–428. doi:10.1061/(ASCE)BE.1943-5592.0000348
- Sim, H. B., and Uang, C. M. (2012). Stress analyses and parametric study on full-scale fatigue tests of rib-to-deck welded joints in steel orthotropic decks. *J. Bridge Eng.* 17 (5), 765–773. doi:10.1061/(ASCE)BE.1943-5592.0000307
- Song, G. B., Gu, H., and Mo, Y. L. (2008). Smart aggregates: Multi-functional sensors for concrete structures—a tutorial and a review. *Smart Mat. Struct.* 17, 033001. doi:10.1088/0964-1726/17/3/033001
- Su, Z. Q., Ye, L., and Lu, Y. (2006). Guided lamb waves for identification of damage in composite structures: A review. *J. sound Vib.* 295, 753–780. doi:10.1016/j.jsv.2006.01.020
- Sun, R., Sevillano, E., and Perera, R. (2015). Debonding detection of FRP strengthened concrete beams by using impedance measurements and an ensemble PSO adaptive spectral model. *Compos. Struct.* 125, 374–387. doi:10.1016/j.compstruct.2015.02.011
- Sun, R., Sevillano, E., and Perera, R. (2017). Identification of intermediate debonding damage in FRP-strengthened RC beams based on a multi-objective updating approach and PZT sensors. *Compos. Part B Eng.* 109, 248–258. doi:10.1016/j.compositesb.2016.10.060
- Talakokula, V., Bhalla, S., and Gupta, A. (2018). Monitoring early hydration of reinforced concrete structures using structural parameters identified by piezo sensors via electromechanical impedance technique. *Mech. Syst. Signal Process.* 99, 129–141. doi:10.1016/j.ymsp.2017.05.042
- Yu, J., Wu, H. L., and Leung, C. K. Y. (2020). Feasibility of using ultrahigh-volume limestone-calcined clay blend to develop sustainable medium-strength Engineered Cementitious Composites (ECC). *J. Clean. Prod.* 262, 121343. doi:10.1016/j.jclepro.2020.121343
- Zhang, Q. H., Cui, C., Bu, Y. Z., Liu, Y. M., and Ye, H. W. (2015). Fatigue tests and fatigue assessment approaches for rib-to-diaphragm in steel orthotropic decks. *J. Constr. Steel Res.* 114, 110–118. doi:10.1016/j.jcsr.2015.07.014
- Zhang, Z., Hu, J., and Ma, H. (2019). Feasibility study of ECC with self-healing capacity applied on the long-span steel bridge deck over-lay. *Int. J. Pavement Eng.* 20 (8), 884–893. doi:10.1080/10298436.2017.1356173
- Zhang, Z., Liu, D., Ding, Y., and Wang, S. (2022). Mechanical performance of strain-hardening cementitious composites (SHCC) with bacterial addition. *J. Infrastruct. Preserv. Resil.* 3 (1), 3–11. doi:10.1186/s43065-022-00048-3
- Zhang, Z., Liu, S., Yang, F., Weng, Y., and Qian, S. (2021). Sustainable high strength, high ductility engineered cementitious composites (ECC) with substitution of cement by rice husk ash. *J. Clean. Prod.* 317, 128379. doi:10.1016/j.jclepro.2021.128379
- Zhang, Z., Yang, F., Liu, J. C., and Wang, S. (2020). Eco-friendly high strength, high ductility engineered cementitious composites (ECC) with substitution of fly ash by rice husk ash. *Cem. Concr. Res.* 137, 106200. doi:10.1016/j.cemconres.2020.106200
- Zhang, Z., Zhang, Q., and Li, V. C. (2019). Multiple-scale investigations on self-healing induced mechanical property recovery of ECC. *Cem. Concr. Compos.* 103, 293–302. doi:10.1016/j.cemconcomp.2019.05.014
- Zhao, S., Fan, S., Yang, J., and Kitipornchai, S. (2020). Numerical and experimental investigation of electro-mechanical impedance based concrete quantitative damage assessment. *Smart Mat. Struct.* 29 (5), 055025. doi:10.1088/1361-665x/ab58e9
- Zhao, Y. J., Jiang, J. W., Ni, F. J., and Zhou, L. (2019a). Fatigue cracking resistance of engineered cementitious composites (ECC) under working condition of orthotropic steel bridge decks pavement. *Appl. Sci. (Basel)*. 9 (17), 3577. doi:10.3390/app9173577
- Zhou, L., Chen, S. X., Ni, Y. Q., and Choy, A. W. H. (2021). EMI-GCN: A hybrid model for real-time monitoring of multiple bolt looseness using electromechanical impedance and graph convolutional networks. *Smart Mat. Struct.* 30 (3), 035032. doi:10.1088/1361-665x/abe292
- Zhu, H. P., Luo, H., Ai, D. M., and Wang, C. (2016). Mechanical impedance-based technique for steel structural corrosion damage detection. *Measurement* 88, 353–359. doi:10.1016/j.measurement.2016.01.041
- Zhu, M. C., Li, X. D., Deng, J., Ye, Z., and Li, J. (2022). Bond degradation and EMI-based monitoring of CFRP to concrete interfaces exposed to wet-dry cycling. *Eng. Struct.* 260, 114225. doi:10.1016/j.engstruct.2022.114225